N O T I C E

THIS DOCUMENT HAS BEEN REPRODUCED FROM MICROFICHE. ALTHOUGH IT IS RECOGNIZED THAT CERTAIN PORTIONS ARE ILLEGIBLE, IT IS BEING RELEASED IN THE INTEREST OF MAKING AVAILABLE AS MUCH INFORMATION AS POSSIBLE

(NASA-TM-82107) FAST PLASMA HEATING BY ANOMALOUS AND INERTIAL RESISTIVITY EFFECTS (NASA) 37 p HC A03/MF A01 CSCL 20I

N81-22914

Unclas
G3/75 21187

NASA

Technical Memorandum 82107

Fast Plasma Heating by Anomalous and Inertial Resistivity Effects

Andre Duijveman, Peter Hoyng, and James A. Ionson

MAY 1981
RECEIVED
NASA STI FACILITY
ACCESS DEPT.

MARCH 1981

National Aeronautics and Space Administration

Goddard Space Flight Center
Greenbelt, Maryland 20771

FAST PLASMA HEATING BY ANOMALOUS AND INERTIAL RESISTIVITY EFFECTS

Andre Duijveman, Peter Hoyng
Space Research Laboratory
Astronomical Institute at Utrecht
The Netherlands

and

James A. Ionson
Laboratory for Astronomy and Solar Physics
NASA/Goddard Space Flight Center
Greenbelt, Md. 20771
USA

IN PRESS, Ap.J.

ABSTRACT

A simple model to describe fast plasma heating by anomalous and inertial resistivity effects is presented. A small fraction of the plasma contains strong currents that run parallel to the magnetic field and are driven by an exponentiating electric field. The anomalous character of the current dissipation is caused by the excitation of electrostatic ion-cyclotron and/or ion-acoustic waves. The possible role of resistivity due to geometrical effects ('inertial resistivity') is also considered. Through the use of a marginal stability analysis, equations for the average electron and ion temperatures are derived and numerically solved. No loss mechanisms have been taken into account. The evolution of the plasma is described as a path in the drift velocity diagram, in which the drift velocity v_D/v_e is plotted as a function of the electron to ion temperature ratio T_e/T_i.

For current layers with dimensions that are large compared to the effective electron mean free path, inertial resistivity is not important and we find that:

(1) Heating due to classical resistivity cannot make $T_e/T_i > 3.1$ before instability sets in. This is always the ion-cyclotron instability.

(2) Whether or not a situation with $T_e/T_i \gg 1$ will occur depends critically on the saturation level of ion-cyclotron waves.

(3) Ion-acoustic wave heating produces a limiting T_e/T_i of 6.4.

If inertial resistivity is important much higher values of T_e/T_i can be attained, because inertial resistivity primarily affects electrons.

The assumption that hard X-rays, emitted during the impulsive phase of a solar flare, are thermal in origin, requires a hot thermal plasma, $T_e \sim 5\times10^8$ K. Our results indicate promising possibilities for the production of such a hot plasma.

Key words: plasma heating - current dissipation - marginal stability - solar flare.

INTRODUCTION

In a plasma, conversion of magnetic energy into heat can take place by current dissipation. Often the heating proceeds slowly so that Coulomb relaxation between electrons and ions keeps the temperatures of both species equal. However if the energy input occurs sufficiently fast, T_e and T_i cease to be equal, since the energy dissipation mechanism favours energization of either electrons or ions, and this is what we wish to study in our present work.

We have two specific interests:

(a) In the plasma-astrophysics literature one often assumes $T_e >> T_i$ on the general grounds that most of the dissipated energy goes into electrons and the electron-ion relaxation time is relatively long (e.g. Kaplan and Tsytovich, 1973). We want to see if this assumption can be justified and if so, what values for T_e/T_i can be attained?

(b) A particular example of rapid plasma heating [1] is the solar flare. It has been found that the hard X-ray emission during the impulsive phase of a solar flare can be attractively explained as thermal bremsstrahlung from a very hot plasma; $T_e \lesssim 5\ 10^8$ K and $T_e >> T_i$ (Brown et al. 1979; Smith and Lilliequist, 1979). The authors quoted take the heating of the plasma for granted and study the subsequent evolution of the hot region situated at the top of a loop, leading to the formation of a conduction front. We wish to concentrate on the mechanisms that are responsible for the rapid plasma heating. Observations indicate that it must occur in a few seconds. The parameters of the numerical case studies that we shall present are all tailored to the flare heating problem.

Rapid conversion of magnetic energy into thermal energy must take place in localized regions, where the current is very concentrated. The reason for this is that a large volume with the same current density everywhere would give rise to unreasonably large magnetic fields at the boundary. Also, because parallel currents attract one another, they tend to clump together (tearing instability; Spicer, 1980; Schnack and Killeen, 1978). We shall refer to these regions of high current density as 'current layers'. They coincide with the surroundings of neutral lines of the (fast) tearing mode configuration and

---

(1) Here and in what follows we understand heating to mean 'bulk energization'. Electron and ion velocity distributions are assumed to be roughly isotropic and Maxwellian.

their large scale spatial distribution can be quite chaotic (Spicer, 1980).

In the current layers the dissipation rate is determined by the magnitude of the current density and the resistivity of the plasma. The latter quantity depends on whether or not the current is unstable to the generation of waves (see for example Papadopoulos, 1977) and on the geometry of the current layers (inertial resistivity). We shall consider electrostatic ion-cyclotron waves, which heat primarily ions, and ion-acoustic waves, which heat primarily electrons. In the presence of these waves we calculate the resistivity by applying the marginal stability analysis concept (Manheimer, 1977; Manheimer and Boris, 1977). In our analysis we shall derive and numerically solve two temperature equations, one for the electrons and one for the ions. Special attention will be paid to the ratio T_e/T_i, because this quantity determines which wavetype has the lower threshold (Kindel and Kennel, 1971).

A difficult question is how the locally high dissipation rates around the neutral lines influence the evolution of the tearing instability. A drastic simplification is necessary. We shall decouple the heating from the evolution of the tearing mode in that we let the electric field in the current layers grow with a constant growth rate.

II. MODEL

We consider a fully ionized hydrogen plasma of volume V, containing a filamentary current distribution. The current layers comprise a fraction ϵ of the volume V and in these current layers there is a strong and growing electric field in the fluid rest frame, virtually parallel to the local magnetic field. In the remaining fraction $1-\epsilon$ the electric field in the fluid frame is assumed to be effectively zero. We define V somewhat loosely as the envelope of the current layers where rapid dissipation takes place. In our discussion the actual size of V is immaterial. The dissipation occurs only

in the fraction ϵ of V and ϵ will be a small number. Though in general a function of time, we shall treat ϵ as a constant. Typically we shall take $\epsilon = 0.01$, without much justification.

If the heat spreads sufficiently fast around the current layers, it is reasonable to introduce one average electron temperature T_e and one average ion temperature T_i in V. Parallel and perpendicular temperatures are taken equal, $T_{e\perp} = T_{e\parallel}$ and $T_{i\perp} = T_{i\parallel}$. These assumptions about T_e and T_i require some further consideration, for which we refer to Appendix I. We shall ignore all energy loss mechanisms from the volume V. These include radiation losses, expansion losses and conduction losses. Though in the case of the solar flare the latter two will certainly be important when the plasma is very hot, we deliberately ignore them in this paper, because we wish to concentrate on the heating mechanisms. We plan to include these loss mechanisms in a later study.

2.1. Dissipated energy and its distribution over electrons and ions

The frictional force that determines the resistivity depends very much on the state of the plasma. If the resistivity is caused by Coulomb collisions, it depends on the electron temperature only. However when the plasma is in a turbulent state, the electrons carrying the current will also interact with the electric field fluctuations in the waves, which changes the resistivity (and other transport coefficients) of the plasma in a way that depends upon the type of waves that grow. As waves that affect the resistivity we shall consider electrostatic ion-cyclotron (IC) and ion-acoustic (IA) waves (c.f., solar applications by Rosner et. al. (1978) and Hinata (1979).

Another factor of importance for the resistivity will be the geometry of the current layers. Fast electrons crossing small current layers will remain under the influence of the electric field only for a short period of time and therefore their contribution to the current density is small. This is due to

the inertia of the electrons. The corresponding resistivity is called inertial resistivity (Speiser, 1970).

Inside the current layers several independent scattering processes i occur at the same time. Thus, the total dissipation rate P_{tot} is related to an effective resistivity η_{EF} as follows:

$$P_{tot} = \eta_{EF} \; j^2 \qquad ; \quad j = ne v_D \tag{1}$$

v_D is the drift velocity corresponding to the current density j. The electric field E and j are related through Ohm's law:

$$E = \eta_{EF} \; j \tag{2}$$

where the total resistivity is the sum of individual contributions:

$$\eta_{EF} = \sum_i \eta_i \tag{3}$$

Four resistivities are distinguished in this paper (see also Appendix IIB):

(a) classical Coulomb resistivity η_{CL}

(b) resistivity due to geometrical effects: inertial resistivity η_{IN}

(c) resistivity due to ion-cyclotron waves: η_{IC}

(d) resistivity due to ion-acoustic waves: η_{IA}.

Because we are interested in the behavior of T_e and T_i, we want to know how the dissipated energy is distributed over electrons and ions. Therefore we introduce the quantity χ_i as the fraction of the dissipated energy $\eta_i \; j^2$ that goes into the electrons by scattering process i. Classical and inertial resistivities energize only electrons (to order $(m/M)^{\frac{1}{2}}$):

$$\chi_{CL} = 1 \qquad ; \qquad \chi_{IN} = 1 \tag{4a}$$

Consequently, without waves, the ions are heated only as a result of classical equilibration, i.e., by the transfer of energy from electrons to ions by electron-ion collisions. However, in the presence of waves, the ions can also gain energy from the waves. In fact, what happens is that the waves act as an intermediary, enabling a transfer of energy from electrons to ions. Thus, despite the fact that the electric field does work only on the electrons, χ_i (i = "IC" or "IA") is found to be less than 1. An expression for χ_i is (Tange and Ichimarum 1974):

$$\chi_i = 1 - \langle \omega \rangle_i / \langle k_\parallel v_D \rangle_i \qquad (4b)$$

where $k_\parallel$ is the component of the wave vector parallel to the magnetic field, ω is the wave frequency and the average is taken over the wave spectrum. Equation (4b) follows from conservation of energy and momentum of particles and waves. Now the dissipated power that goes into electrons (P_e) and ions (P_i) is

$$P_e = \sum_i \chi_i \eta_i j^2 \quad ; \quad P_i = \sum_i (1 - \chi_i) \eta_i j^2 \qquad (5)$$

With expressions for η_i and χ_i as a function of the drift velocity v_D, the wave level w_i and the wave spectrum $\omega_i(\underline{k})$ it is possible, in principle, to calculate the above dissipation rates P_e and P_i. Because in general the wave level and wave spectrum are not known a priori, we must follow a special procedure that is outlined in the next section.

2.2 Marginal stability analysis

Recently, a method has been developed which enables one to derive values for the transport coefficients of a plasma in a turbulent state, without solving any microscopic equations (Manheimer and Boris, 1977; Manheimer, 1977). The

method uses the fact that an unstable plasma evolves toward a marginally stable state and has already been successfully applied to computing laboratory plasma problems (Kalfsbeek, 1978; and references cited in Manheimer and Boris, 1977). In this paper we shall use the marginal stability analysis only for computing the plasma resistivity and its essence is as follows. Suppose we start with a small current so that dissipation is governed by Coulomb collisions only. From an analysis of the linear dispersion relation (see Appendix IIA and for example Kindel and Kennel, 1971) one can find the minimum drift velocity for which the current parallel to the magnetic field becomes unstable. One sees (Figure 1A) that for a plasma with $T_e/T_i < 8$, ion-cyclotron waves have the lowest threshold. The critical drift velocity is denoted with v_{IC}. Therefore, if the current density grows, the plasma will first become ion-cyclotron unstable. As long as the ion-cyclotron waves are not saturated, the drift velocity v_D remains approximately equal to v_{IC} and thus it is possible to calculate the effective resistivity from

$$\eta_{EF} = E/j_{IC} \quad ; \quad j_{IC} = ne\,v_{IC} \tag{6}$$

From this and from $\eta_{EF} = \eta_{CL} + \eta_{IC}$ one can calculate η_{IC}.

Figure 1A,B

The energy density of the waves w_{IC} can now be computed from an expression for η_{IC} as a function of the wave level (see Appendix IIB, formula (B7)). Next compare this wave level w_{IC} with the saturation wave level w^s_{IC} for ion-cyclotron waves. If $w_{IC} < w^s_{IC}$, the assumption of marginal stability is correct.

As soon as the waves saturate, the current density starts to deviate from j_{IC} for ion-cyclotron waves and increases till the instability with the next

lowest threshold sets in. This is the ion-acoustic instability. Again the plasma evolves toward the marginally stable state, this time with j remaining close to j_{IA} for ion-acoustic waves (see Figure 1A).

Apart from the resistivity, the marginal stability analysis also provides the frequency and the wave vector around which the wave spectrum is peaked and thus enables one to calculate χ_i (i = 'IC' or 'IA') from equation (4b). For the details of this we refer to Appendix IIA and the references cited there. A graph of χ_i as a function of T_e/T_i is displayed in Figure 1B. If the ion-cyclotron waves are saturated, calculation of χ_{IC} becomes more difficult (see Appendix IIC). For this case, the calculation of v_D follows from Figure 2.

From the above discussion it follows that the heating process consists of a number of successive stages. The switch-over from one stage to the next is determined by the threshold and the saturation level of the waves. We have summarized this in a block diagram, see Figure 2. It is unfortunate that the wave levels cannot be determined very reliably, despite the decisive role they play in the computation.

Figure 2

2.3 Equations

Electron-and ion-heating and the growth of the electric field are described by the following equations:

$$\frac{3}{2} n k_B \frac{dT_e}{dt} = - \frac{3}{2} n k_B \frac{T_e - T_i}{\tau_{eq}} + \varepsilon \sum_i \chi_i n_i j^2 \qquad (7a)$$

$$\frac{3}{2} n k_B \frac{dT_i}{dt} = \frac{3}{2} n k_B \frac{T_e - T_i}{\tau_{eq}} + \varepsilon \sum_i (1 - \chi_i) n_i j^2 \qquad (7b)$$

$$\frac{dE}{dt} = \gamma E \qquad (7c)$$

with

$$\eta_{EF} = \sum_i \eta_i \quad ; \quad j = E/\eta_{EF} \tag{8a}$$

$$\tau_{eq} = \frac{3}{8(2\pi)^{\frac{1}{2}}} \frac{1}{\ln \Lambda} \frac{m M}{n e^4} \left(\frac{k_B T_e}{m}\right)^{3/2}, \tag{8b}$$

τ_{eq} is the electron-ion equilibration time (Sivuhkin, 1966), γ is the growth rate of the electric field. We assume γ to be a constant. The first term on the right hand side of the temperature equations describes heat exchange between electrons and ions by classical Coulomb collisions. Note that it does not contain a factor ϵ because classical equilibration takes place everywhere outside the current layers.

We now introduce the following dimensionless variables:

$$T_e' = T_e/T_{e,o} \quad ; \; T_i' = T_i/T_{e,o} \quad ; \quad E' = E/E_o \quad ; \; t' = t/\tau_H(o) \tag{9}$$

The subscript zero denotes values at time $t = o$ and

$$\tau_H(t) = \frac{1.5\, n\, k_B T_e}{E^2/\eta_{CL}} \tag{10}$$

$\tau_H(o)/\epsilon$ is the characteristic electron heating time at $t = o$. In terms of the new variables the equations read (we drop the primes):

$$\frac{dT_e}{dt} = -\alpha \frac{T_e - T_i}{T_e^{1.5}} + \epsilon\, \chi_{EF}\, E^2/\eta_{EF} \tag{11a}$$

$$\frac{dT_i}{dt} = \alpha \frac{T_e - T_i}{T_e^{1.5}} + \epsilon\, (1 - \chi_{EF})\, E^2/\eta_{EF} \tag{11b}$$

$$\frac{dE}{dt} = \gamma E \tag{11c}$$

with

$$\eta_{EF} = \sum_i \eta_i \quad ; \qquad \chi_{EF} \equiv \sum_i (\eta_i / \eta_{EF})\, \chi_i \tag{12a}$$

$$\eta_{EF} = (6/\alpha)^{\frac{1}{2}} \; (m/M)^{\frac{1}{2}} \; (v_e/v_D) \; E/T_e^{\frac{1}{2}} \tag{12b}$$

$$\alpha \equiv \frac{\tau_H(o)}{\tau_{eq}(o)} = \frac{1}{3\pi} \frac{m}{M} \left(\frac{E_D(o)}{E_o} \right)^2 \quad ; \; E_D(o) = \frac{4\pi n e^3 \ln\Lambda}{k_B T_{e,o}} \; . \tag{12c}$$

(12b) is just the relation $\eta_{EF}=E/j$ from (8a), re-expressed in the dimensionless units (9).

It so happens that the dimensionless constant α can be written in terms of the ratio of the initial electric field and the initial Dreicer field $E_D(o)$. All η's are expressed in units of $\eta_{CL}(o)$, the classical resistivity at $t = o$. The growth rate γ in equation (11c) is dimensionless and expressed in units of $\tau_H^{-1}(o)$. v_e is the electron thermal speed, $v_e = (k_B T_e/m)^{\frac{1}{2}}$.

III. RESULTS

In this section we shall present some scenarios of fast plasma heating computed from eq. (11a-c). At $t = o$ we always have equal electron and ion temperatures. We shall start with an investigation of the classical heating phase. Next we will choose a specific set of parameter values and show numerically how the plasma evolves in the other heating stages as well.

3.1. Classical heating

In stage 1, $\chi_{EF} = 1$ and $\eta_{EF} = T_e^{-1.5}$ (dimensionless units). Addition of (11a) and (11b) gives

$$\frac{d}{dt}(T_e + T_i) = \varepsilon T_e^{3/2} E^2 \quad ; \quad E = \exp(\gamma t) \tag{13}$$

It is easy to solve eq. (13) for two limiting cases. The first case is strong electron-ion equilibration which keeps T_e and T_i equal. The second limiting

case happens if the transfer of energy from electrons to ions by Coulomb collisions is negligible. In both cases the temperature growth is explosive (Coppi and Friedland, 1971). More interesting than the temperature growth itself is the behavior of the temperature ratio T_e/T_i during classical heating. We found that the explosive temperature growth does not automatically lead to large T_e/T_i. The reason for this is that before T_e/T_i starts to deviate considerably from unity, the plasma becomes electrostatically unstable. The larger the electric field is the lower the electron and ion temperatures at which the plasma becomes unstable. Therefore $(T_e/T_i)_{cr}$, the value of T_e/T_i at instability onset, decreases with increasing growth rate of the electric field. In Figure 3 we have plotted $(T_e/T_i)_{cr}$ as a function of the growth rate of the electric field for three different filling factors ϵ. The instability is always the ion-cyclotron instability. Obviously $(T_e/T_i)_{cr}$ is largest for $\gamma = 0$ and $\epsilon = 1$, when it reaches the value 3.1. Therefore it is impossible to make $T_e/T_i > 3.1$ by classical Coulomb dissipation in a plasma with an exponentially growing electric field. As we shall show in the next section, the subsequent evolution of the plasma after instability onset, is not necessarily toward large T_e/T_i. This is due to the fact that ion-cyclotron waves preferentially heat the ions. Therefor we cannot confirm the conclusion of Rosner et al (1978) that a large T_e/T_i can be easily produced. They reached this conclusion by their assumption that after the classical heating phase the two-stream (i.e. Buneman) and ion-acoustic instability will be excited. This is not true because the ion cyclotron instability has a lower threshold.

3.2. Results including anomalous heating (no inertial resistivity)

We shall now present some scenarios of fast plasma heating. With this aim we choose the following dimensionless parameters:

$$\alpha = 5 \; ; \quad \varepsilon = 0.01 \; ; \quad \gamma = 10 \tag{14}$$

Eqs. (11a-c) depend at first sight only on the constants specified in (14). In reality, the density, magnetic field etc. all enter because the marginal stability analysis requires us to compute wave energy densities and to switch stages on the basis of this. Therefore we extend (14) with parameters appropriate for impulsive heating as it is assumed to occur in solar flares (Brown et al., 1979; Smith and Lilliequist, 1979):

$$n = 10^{11} \text{ cm}^{-3} \; ; \quad B = 500\,\text{G} \; ; \quad T_{e,o} = T_{i,o} = 5\ 10^{6} \text{ K} \tag{15}$$

The density and the magnetic field are kept constant; the Coulomb logarithm is also kept constant, equal to 20. The above parameters imply a classical heating phase first, because at t = 0 we have $v_D/v_{IC} = 0.05$ and $v_D/v_{IA} = 0.02$. With (14) and (15) we find

$$\tau_{eq}(o) = 1.4\,\text{s} \; ; \; \tau_H(o) = 7.1\,\text{s} \; ; \; E_o/E_D(o) = 0.003 \; ; \; E_D(o) = 10^{-3} \text{ V cm}^{-1} \tag{16}$$

We terminate the computation as soon as $T_e = 100$ (i.e. $5\ 10^8$ K). The growth time of the electric field is $\tau_H(o)/\gamma$ or 0.7 s. In all scenarios considered below, increase of T_e by two orders of magnitude takes place in approximately 7 or 8 growth times, that is in about 5 s, while increase of T_e from $5\ 10^7$ to $5\ 10^8$ K happens in 1 or 2 growth times, or about 1 s. We defer all discussion on application to the flare heating problem to the next section.

Figure 4,5
on left page

Figure 6,7
on opposing right

In stage 2 the presence of ion-cyclotron waves keeps the plasma in a marginally stable state. From Figure 1B we see that ion-cyclotron waves preferentially heat ions. Therefore they tend to decrease the ratio T_e/T_i while classical resistivity still tends to increase T_e/T_i. If the resistivity due to ion-cyclotron waves starts to dominate classical resistivity, the ratio T_e/T_i will drop. Whether this will happen or not depends on the saturation level of the waves. Unfortunately, this saturation level is not well known. Therefore we consider three different saturation levels (see also Appendix IIC).

(1) a low saturation level due to plateau formation (Petviashvili, 1964), strictly valid for an infinite homogeneous plasma only. In this case the maximum contribution of the ion-cyclotron waves to the resistivity is of the order of the classical resitivity.

(2) a high saturation level due to ion resonance broadening (Palmadesso et al., 1974). From (C2) we find that w_{IC}^s is approximately equal to 1, sometimes even larger than 1. For this reason we preferred to simulate saturation by ion resonance broadening by taking a fixed $w_{IC}^s = 0.5$. In this case, the resistivity due to ion-cyclotron waves soon dominates classical resistivity

(3) An intermediate saturation level, $w_{IC}^s = 0.01$.

Note that all our wave energy densities include both the electrostatic and the kinetic part. Therefore, because the resistivity is determined by the electrostatic energy density only, equal total energy densities in ion-cyclotron and ion-acoustic waves can give resistivities that are quite different. The wave levels for ion-acoustic waves that occur in our computations, are always low, so that they will not saturate. We will not pay much attention to the behaviour of the electron and ion temperatures themselves as a function of time. We found it to be much more interesting to follow the evolution of the plasma in Figure 1A, the drift velocity diagram. Though a point in this diagram does not completely specify the state of the plasma, it shows which wave types are present and how the energy is distributed over electrons and ions. A part of the evolutionary paths coincides with the marginal stability curves (it is somewhat like the Hertzsprung-Russell diagram with evolutionary paths). The drift velocity diagram shows the stages, defined in Figure 2, through which the plasma goes during the heating process. For the three saturation levels mentioned above, we have calculated the evolutionary paths in the drift velocity diagram. The results are displayed in Figure 4. For the low saturation level

-case 1- we illustrate the temperatures T_e and T_i, the fraction χ_{EF} of the dissipated energy going into electrons, the resistivities (η_{CL}, η_{IC}, η_{EF}) and the wave levels (w_{IC}, w_{IA}) as a function of time (Figure 5). In Figure 4B the plasma goes through stage 1 and ends in stage 2 with $T_e/T_i \sim 0.3$ and $w_{IC} \sim 0.15$. The ion-cyclotron waves that dominate the heating process apparently never saturate. In Figure 4C the plasma goes through stage 1, excites ion-cyclotron waves (stage 2) that saturate (stage 3) and stays in stage 3 till the end of the computation ($T_e \sim 100$); then $T_e/T_i \sim 1.1$. The reason for T_e/T_i to remain close to unity in stage 3 is that the fraction of the dissipated energy that is put into the electrons by the waves increases the further the drift velocity is above the ion-cyclotron critical drift velocity v_{IC} (Appendix IIC, eq. (C3)). In both Figures 4B and 4C the increasing resistivity due to ion-cyclotron waves prevents the fast growth of the current density to the ion-acoustic threshold. In Figure 4A ion-cyclotron waves saturate at such a low level that they are not important for the final evolution of the plasma. The growing electric field drives the plasma ion-acoustically unstable (stage 4) and the plasma evolves along the marginal stability curve for ion-acoustic waves to the right in the drift velocity diagram. That is the electrons are preferentially heated and we end with $T_e/T_i \sim 6.3$. The fact that T_e/T_i stabilizes at about this value when ion-acoustic waves are dominant can be easily explained (Kalfsbeek, 1978). With eqs. (11a,b), ignoring all terms except the ion-acoustic one, we find

$$\dot{T}_e/\dot{T}_i = \chi_{IA}/(1 - \chi_{IA}) , \tag{17}$$

With the help of equation (A8) and the introduction of $x = T_e/T_i$ we find for $x > 6$:

$$dx/d(\ln T_e) = x - (m/M)^{\frac{1}{2}} x^{\frac{3}{2}} \exp(0.5x + 1.5). \tag{18}$$

It follows that x always approaches the value for which the r.h.s. of eq. (18) vanishes, that is T_e/T_i approaches the limit 6.4. This value only depends on M/m. If energy losses are included, this value 6.4 will probably become lower.

3.3. Inertial resistivity

We now want to discuss how the size of the current layers influences the heating process. We assume that the electrons outside the current layers have a Maxwellian distribution. The electrons that enter the current layers with a (thermal) velocity parallel to the electric field are decelerated (they lose energy), while the electrons with a (thermal) speed in the opposite direction are accelerated (they gain energy). Because the gain is somewhat larger than the loss, the net result is an increase in the energy of the electrons. The directed energy they gain in this way is randomized in between the current layers by Coulomb collisions and by scattering off chaotic magnetic fields. Therefore, the effect of inertial resistivity is to heat the electrons in volume V. Of course, inertial resistivity will only be important if the time during which a thermal electron crosses a current layer is of the order of, or less than a typical (effective) collision time. This means that current layers with a characteristic length scale L (see Appendix IIB) smaller than the effective mean free path of an electron will carry a current that is determined mainly by inertial effects. Inertial resistivity heats only electrons (to order $(m/M)^{\frac{1}{2}}$) and hence its effect is to increase T_e/T_i, offering the possibility of quite different paths in the drift velocity diagram, see Figure 6. Three different length scales will be considered, namely L = 1, 3 and 10 km. For the L = 1 km case the influence of inertial resistivity is most obvious, because here T_e/T_i has increased till just above 8 while still in stage 1 so that ion-acoustic waves are the first to be generated and the saturation level of ion-cyclotron waves is irrelevant. For L = 10 km, $w_{IC}^s = 0.5$, inertial resistivity is less dominant and ion-cyclotron waves are generated first. However, instead of moving along the ion-cyclotron marginal stability curve to the left as in Figure 4B without inertial resistivity,

the plasma now evolves to the right along this curve. For the intermediate case L = 3 km, $w_{IC}^{s} = 0.01$, again ion-cyclotron waves are generated first. However, they quickly saturate and soon ion-acoustic waves are excited. For this intermediate case, inertial resistivity is also important in stage 4 as is illustrated by the fact that T_e/T_i increases above 6.4. In Figure 7 we also show the temperature, x_{EF}, resistivities and wave levels for this case.

IV. DISCUSSION

4.1. Summary of behavior of T_e/T_i during the heating

Though in principle classical heating could make $T_e >> T_i$, this never happens because the current becomes unstable before T_e/T_i attains high values. The maximum value that we found at instability onset was 3.1. There appear to be two possibilities for the production of a plasma with $T_e >> T_i$. The first is that the ion-cyclotron waves saturate at a low level, so that ion-acoustic waves will be excited. Then T_e/T_i will stabilize at 6.4. The second possibility is that because of the small dimensions of the current layers, inertial resistivity is important. In that case, large T_e/T_i can be obtained even for high saturation levels of the ion-cyclotron waves.

4.2. Application to solar flare problem

If the observed hard X-rays from the solar flare plasma are interpreted as thermal bremsstrahlung, it is readily calculated that a plasma with an electron temperature of about 5×10^{8}K (corresponding to 43 keV) and a volume $V \sim 10^{23}$ cm^3 (corresponding to an emission measure $\int n^2 dV = 10^{45}$ cm^{-3} when $n = 10^{11}$ cm^{-3}) is necessary. This hot plasma must be produced fast (in a few seconds) because heat conduction will prevent a slow temperature rise to 5×10^{8}K. Therefore, for all cases that we have presented, we used a fixed growth time of the electric field of 0.7 s so that we get just about the

required heating time. Not all the possibilities treated in this paper are equally suitable as a mechanism for impulsive electron heating. T_e/T_i increases considerably above unity, we expect that the neglect of expansion losses can be justified during a large part of the heating process. Otherwise, shock formation and disruption of the tearing mode structure might occur. Also, the anomalous heat conduction front theory (Brown et al, 1979; Smith and Lilliequist, 1979) has been carried out only under the assumption $T_e/T_i \gg 1$, so that it is uncertain if in the case $T_e/T_i \sim 1$ the thermal model emits hard X-rays more efficiently than the beam target models (Brown, 1971). If it does not, the main advantage of the thermal model namely the gain in radiation efficiency, disappears. In 4.1 it is summarized under what circumstances a plasma with $T_e \gg T_i$ is produced.

4.3. Exponentiating electric field

A drawback of our work is the absence of any coupling between heating and the evolution of the tearing mode. One might even argue that a factor 100 increase in T_e in approximately 5 s as illustrated in the numerical examples is meaningless because an exponentiating electric field eventually produces any desired heating. This is true but it must be realized that the largest electric field that we used is only about 5×10^{-3} V/cm, which is very small compared to the maximum electric field available, E_{max}. The latter can be estimated as $\underline{E}_{max} = \underline{v} \times \underline{B}/c \sim 170$ V/cm, where $v \sim 0.1\ B/(4\pi nM)^{\frac{1}{2}}$, B = 500 G and $n = 10^{11}$ cm^{-3}. In practice $\underline{E}_{max}$ will be smaller because of neglect of angular factors, but it will certainly be much larger than 5×10^{-3} V/cm. Apparently we have quite some freedom to use larger electric fields. We may need these larger fields to produce $T_e \sim 5\times10^8$K if losses are included or if, for example, ϵ is much smaller than 0.01.

In our calculations we did not take into account electron runaway. Comparing E with the classical Dreicer field E_D (formula 12c), we find that at $t = 0$ the ratio $E/E_D \sim 3\times10^{-3}$ while at the end of the run $E/E_D \sim 500$. However, whether or not electron runaway occurs in the current layers depends on an effective Dreicer field $E_{D,EF}$, which differs from the classical Dreicer field in that the classical collision frequency is replaced by an effective collision frequency $\nu_{EF} = (ne^2/m)\eta_{EF}$. With $E_{D,EF} = (mv_e/e)\,\nu_{EF}$, it is easy to show that $E/E_{D,EF} = v_D/v_e \leq 1$. Neglecting electron runaway is justified along most of the evolutionary path in Figure 4. In the case that inertial resistivity is important, Figure 6, the small size of the current layers prevents electrons from running away.

4.4. Slowly changing total resistivity

The behavior of the total resistivity (c.f., Figures 5B and 7B) contradicts the popular view in that it jumps discontinuously by many orders of magnitude. The essence of the marginal stability analysis is that the time scale for changes in the effective resistivity (and all other transport coefficients) is reduced to the MHD evolution time. In our case, the final resistivity is between one and two orders of magnitude larger than at $t = o$. Of course, the classical resistivity decreases a factor 1×10^3 since $\eta_{CL} \propto T_e^{-1.5}$ and T_e increases by 100. Hence one might say that a factor 10^4 to 10^5 in resistivity is gained. Note that this happens only in the current layers, not in the bulk of the plasma.

ACKNOWLEDGMENT

The authors benefitted considerably from their participation to the CECAM Workshop on Physics of Solar Flares, where this work has started. In particular we acknowledge helpful discussions with Drs. D. S. Spicer and J. Heyvaerts.

APPENDIX I

Heat conduction around current layers; temperature isotropy and homogeneity.

With the parameters that we use for the solar flare ($n \sim 10^{11}$ cm^{-3}; $T_e \sim T_i \sim 5 \times 10^6$K in the initial phase, see (15)), we find that the mean free path for electrons as well as ions is about 10 km. Because we expect the current layers to have a typical transverse length scale of a few kilometers, we must assume that heat transport from the dissipation regions is non-classical. Ion heat transport parallel to the magnetic field will then take place with approximately the ion thermal speed (convection) which is a hundred kilometers per second or more ($T_i > 5 \times 10^6$K). This is enough to explain the ion-temperature uniformity parallel to the magnetic field during the heating. In the same way we can argue that the electron temperature will be uniform along the magnetic field. Perpendicular to the magnetic field the situation is more difficult. The classical heat conductivity is reduced considerably for both the electrons and the ions. However , in the presence of ion-cyclotron waves, the ion perpendicular heat conduction is strongly enhanced (Ionson et. al., 1979). Thus, within the current layers where ion-cyclotron turbulence is present, ion perpendicular heat conduction is relatively efficient. Note that heat flow away from the current layers is primarily along the magnetic field. However, the magnetic field structure itself is probably quite chaotic (e.g., through the effects of tearing instabilities) thereby enabling the particles to distribute thermal energy throughout the volume V by simply following the field lines. Differences in $T_{i\perp}$ and $T_{i\parallel}$ as well as in $T_{e\parallel}$ and $T_{e\perp}$ may in principle develop. For instance ion-cyclotron waves increase $T_{i\perp}$ rather than $T_{i\parallel}$ (Dakin, 1976, Ionson, 1979). However, temperature anisotropies will drive fast electromagnetic instabilities (Davidson, 1972 Ch. 10,11,12; Davidson and Ogden, 1975), that maintain isotropy, both for electrons and ions.

APPENDIX II

A. The calculation of v_{IC}, v_{IA}, χ_{IC} and χ_{IA} under marginally stable conditions.

The critical drift velocity is obtained as follows. With the linear dispersion relation, the growth rate $\bar{\gamma}$ of the waves can be determined as a function of v_D and of the wave vector $\underline{k}$. For small v_D, $\bar{\gamma}$ is negative for every $\underline{k}$ and all waves are damped. With increasing v_D, the growth rate γ will increase. The v_D for which the maximum of $\bar{\gamma}(\underline{k})$ equals zero is the critical drift velocity. Together with the corresponding wave vector, it can be found from:

$$\bar{\gamma} = o \quad ; \quad \frac{\partial \bar{\gamma}}{\partial \underline{k}} = o \tag{A1}$$

If T_e/T_i is not too different from 1, an approximate expression for the growth rate is (Lee, 1972):

$$\bar{\gamma} = -\sqrt{\pi} \cdot \frac{\Delta^2}{\Gamma_1} \Omega \left\{ \frac{T_i}{T_e} \left(\frac{\omega - k_{\parallel} v_D}{\sqrt{2}\, k_{\parallel} v_e} \right) + \Gamma_1 \left(1 + \frac{1}{\Delta}\right) \rho \exp\left(-\rho^2\right) \right\} \tag{A2}$$

where

$$\Delta = \frac{\omega(k) - \Omega}{\Omega} = \frac{\Gamma_1}{1 - G + T_i/T_e}$$

$$\Gamma_n = e^{-\mu} I_n(\mu); \quad \mu = \frac{k_{\perp}^2 v_i^2}{\Omega^2} \; ; \; v_i^2 = \frac{k_B T_i}{M} \; ; \; v_e^2 = \frac{k_B T_e}{m} \tag{A3}$$

$$G(\mu) = \Gamma_1(\mu) + \frac{1 - \Gamma_o}{\mu} \; ; \; \Omega = \frac{e B}{M c}$$

$$\rho = \frac{\omega - \Omega}{\sqrt{2}\, k_{\parallel} v_i}$$

I_n is the modified Bessel function of order n. The condition $\bar{\gamma} = o$ gives (Lee, 1972):

$$\frac{v_D}{v_e} = \sqrt{2}\,(1+\frac{1}{\Delta})\rho\left(\frac{T_i}{T_e}\right)^{1/2}\left[\sqrt{\frac{m}{M}}+\left(\frac{T_e}{T_i}\right)^{3/2}\Gamma_i\, e^{-\rho^2}\right] \qquad (A4)$$

Minimizing the above expression with respect to ρ and μ is equivalent to (A1) and in this way v_{IC} is found. The values of Δ and ρ for which (A3) is minimized can be used to calculate χ_{IC} with (4b):

$$\chi_{IC} = 1 - (2m/M)^{\frac{1}{4}}\,(T_i/T_e)^{\frac{1}{4}}\rho\,(1+1/\Delta)\,(v_e/v_{IC}) \qquad (A5)$$

For Δ we found the following fit

$$\Delta = \begin{cases} 0.1(5\,T_e/T_i - 2.1)^{\frac{1}{2}} & T_e/T_i \geq 1. \\ 0.01 + 0.16\,T_e/T_i & T_e/T_i < 1. \end{cases}$$

The values of ρ that we used, can be retraced with the help of (A5), the fit for Δ and Figures 1A and 1B .

For ion-acoustic waves we took for $T_e/T_i < 6$, the critical drift velocity v_{IA} as given by the graph of Fried and Gould (1961). This graph is also reproduced in Kindel and Kennel (1971). For larger values of T_e/T_i we used an analytical expression (Krall and Trivelpiece 1973, Chapter 9):

$$v_{IA}/v_e = (m/M)^{1/2} + (T_e/T_i)^{3/2}\exp(-0.5\,T_e/T_i - 1.5) \qquad \text{for } T_e/T_i > 6 \qquad (A6)$$

With the help of (4b), Kindel and Kennel (1971) and (A6) we find:

$$\chi_{IA} = \left(1 + (m/M)^{\frac{1}{4}}\right)^{-1} \qquad \text{for } T_e/T_i \lesssim 1 \qquad (A7)$$

$$\chi_{IA}/(1-\chi_{IA}) = (M/m)^{1/2}\,(T_e/T_i)^{3/2}\exp(-0.5\,T_e/T_i - 1.5) \qquad \text{for } T_e/T_i > 6 \qquad (A8)$$

where we also used that $\omega/k_{\parallel} \approx (m/M)^{\frac{1}{2}} v_e$ for large T_e/T_i. For T_e/T_i between 1 and 6, an expression for χ_{IA} was obtained by linear interpolation.

B. Resistivities

The following expressions for classical and inertial resistivity have been used:

(a) For classical resistivity (Spitzer, 1962):

$$\eta_{CL} = (8\pi/9)^{1/2} \; m^{1/2} \; e^2 \; \ln\Lambda \; (k_B T_e)^{-3/2} \tag{B1}$$

(b) For inertial resistivity we start from the general expression $\eta = 4\pi(\omega_e{}^2\tau)^{-1}$ (Papadopoulos, 1977), where $\omega_e = (4\pi \; n \; e^2/m)^{\frac{1}{2}}$ is the electron plasma frequency. Usually τ is the characteristic scattering time, but now we set τ equal to L/v_e, the average time that an electron stays inside the current layer of characteristic dimension L (Speiser, 1970):

$$\eta_{IN} = \frac{m}{ne^2} \; \frac{v_e}{L} \tag{B2}$$

Note that if the current layer is very elongated, L is of the order of the transverse dimension of the current layer. The reason is that $\underline{B}$ will cross the current layer at some angle ($\underline{E}$ and $\underline{B}$ are not necessarily parallel), so that a particle will cross the current layer by just following a field line.

The resistivity due to electrostatic wave turbulence is derived from the relation (Tange and Ichimaru, 1974, Papadopoulos, 1977):

$$\eta = - \frac{1}{\omega_e} \; \frac{1}{n k_B T_e} \; \frac{v_e}{v_D} \int \frac{d^3\underline{k}}{(2\pi)^3} \int d\omega \cdot k_{\parallel} \lambda_e < E^2 | \underline{k}, \omega > \; \mathrm{Im} \; \chi_e \tag{B3}$$

where $\lambda_e = v_e/\omega_e$ is the electron Debye length and

$$w = \frac{1}{n k_B T_e} \int \frac{d^3\underline{k}}{(2\pi)^3} \int d\omega \, < E^2 | \underline{k}, \omega > \qquad (B4)$$

is the electrostatic wave energy density normalized to $n k_B T_e$.

The electronic susceptibility χ_e is given by (Ichimaru, 1973; Davidson, 1972):

$$\mathrm{Im}\,\chi_e = - \frac{\pi \omega_e^2}{k^2} \sum_n \int d^3\underline{v} \left[\frac{n\Omega}{v_\perp} \frac{\partial}{\partial v_\perp} + k_\parallel \frac{\partial}{\partial v_\parallel} \right] f_e(\underline{v}) J_n^2 \, \delta(k_\parallel v_\parallel - \omega - n\Omega) \qquad (B5)$$

The argument of the Bessel function J_n is $k_\perp v_\perp/\Omega$. We now make the following assumptions:

(1) only the n = o resonance contributes because for ion-cyclotron waves $k_\perp v_\perp / \Omega << 1$ and for ion acoustic waves $k_\perp \sim o$
(2) $f_e(v)$, the electron velocity distribution function is a drifting Maxwellian with v_D parallel to $\underline{B}$.
(3) $|\omega - k_\parallel v_D| < k_\parallel v_e$

Then we find for both wave types:

$$\eta \simeq \left(\frac{\pi}{2}\right)^{\frac{1}{2}} \frac{v_e}{v_D} < \frac{k_\parallel v_D - \omega}{(k \lambda_e)^2} > \frac{w}{\omega_e^2} \qquad (B6)$$

For the plasma in a marginally stable state we approximate $< (k_\parallel v_D - \omega)/(k \lambda_e)^2 >$ as $(k_\parallel v_D - \omega)/(k \lambda_e)^2$, where $k_\parallel$ and ω are those of the marginally stable wave. The factor $(k \lambda_e)^{-2}$ is awkward, in particular for ion-acoustic waves which have formally $k = o$ for the marginally stable wave (Fried and Gould, 1961). We eliminate $(k \lambda_e)^{-2}$ by using <u>total</u> (electrostatic + mechanical) wave energy densities. Without proof we mention, for $k \lambda_e << 1$:

$$\frac{\partial}{\partial\omega}(\omega\epsilon) \simeq \begin{cases} (k\lambda_e)^{-2}\left[1 + \frac{T_e}{T_i}(1 - G + \Gamma_1/\Delta^2)\right] & \text{for IC} \\ 2(k\lambda_e)^{-2} & \text{for IA} \end{cases}$$

(ϵ is the dielectric coefficient). This then leads to:

$$\text{(c)} \quad \eta_{IC} = \left(\frac{\pi}{2}\right)^{\frac{1}{2}} \frac{1}{\omega_e^2} \frac{v_e}{v_D} w_{IC} \frac{k_\parallel v_D - \omega}{1 + \frac{T_e}{T_i}(1 - G + \Gamma_1/\Delta^2)} \tag{B7}$$

$$\text{(d)} \quad \eta_{IA} = \frac{1}{2}\left(\frac{\pi}{2}\right)^{\frac{1}{2}} \frac{1}{\omega_e^2} \frac{v_e}{v_D} w_{IA} (k_\parallel v_D - \omega) \tag{B8}$$

where w_{IC} and w_{IA} are <u>total</u> energy densities. Finally, $k_\parallel v_D - \omega$ is rewritten in terms of χ, as follows:

$$k_\parallel v_D - \omega = \frac{k_\parallel v_D - \omega}{\omega}\,\omega \simeq \begin{cases} \frac{\chi_{IC}}{1 - \chi_{IC}}(1 + \Delta)\,\Omega & \text{for IC} \quad \text{(B9)} \\ \frac{\chi_{IA}}{1 - \chi_{IA}}\left(\frac{m}{M}\right)^{\frac{1}{2}} \omega_e & \text{for IA} \quad \text{(B10)} \end{cases}$$

C. <u>Saturation of ion-cyclotron waves</u>

In an infinite homogeneous plasma, saturation of ion-cyclotron waves occurs at a low level due to the formation of a plateau in the electron distribution function. The contribution of the saturated ion cyclotron waves to the resistivity then is (Petviashvili, 1964):

$$\eta_{IC}^{s} = \eta_{CL} \frac{v_D}{v_e} \tag{C1}$$

However, due to spatial inhomogeneity of the plasma, it is quite possible that ion resonance broadening will be the non-linear process that saturates the instability. In that case the saturation level (electrostatic + kinetic) is much higher and is given by (Palmadesso et al., 1974):

$$w_{IC}^{s} = 2 \left[1 + \frac{T_e}{T_i} (1 - G + \Gamma_1/\Delta^2) \right] \left(\frac{T_i}{T_e} \right)^2 \Delta^2 \qquad (C2)$$

We assume that the wave level corresponding to η_{IC}^{s} from (C1) and the resistivity η_{IC}^{s} corresponding to (C2) can be calculated with the help of equation (B7).

Let us assume that in the saturated state the wave spectrum is still peaked about the wave vector where the growth rate of formula (A2) has a maximum. Introduction of the variable $y = \omega/(\sqrt{2}\, k_{\parallel} v_e)$ in (A2), so that $\rho = (M/m)^{\frac{1}{2}} (\Delta/(1+\Delta)) (T_e/T_i)^{\frac{1}{2}} y$, teaches us that for a given T_e/T_i and Δ, the derivative $\frac{\partial}{\partial y} (\gamma/\Omega)$ is a function of y only and does not depend on v_D/v_e. Because for the maximum growth rate $\left[\frac{\partial}{\partial y} (\bar{\gamma}/\Omega)\right]_{y = y_{max}} = 0$, the value of y_{max} does not depend on v_D/v_e, or, equivalently, $(\omega/k_{\parallel} v_e)$ is a constant for T_e/T_i fixed. In the saturated state we thus have, starting from (4b):

$$\chi_{IC}^{s} = 1 - (\omega/k_{\parallel} v_e) (v_e/v_D) = 1 - \text{const.}\ (v_e/v_D) = 1 - (1 - \chi_{IC})\ (v_{IC}/v_D) \qquad (C3)$$

where the constant has been found by requiring $\chi_{IC}^{s} = \chi_{IC}$ if $v_D = v_{IC}$. Formula (C3) implies that as v_D increases above v_{IC} a progressively larger fraction χ_{IC}^{s} of the turbulently dissipated energy goes into the electrons.

REFERENCES

Brown, J.C.: 1971, Solar Physics 18, 489.

Brown, J.C., Melrose, D. and Spicer, D . S.: 1979, Ap. J. 228, 592.

Coppi, B. and Friedland, A.B.: 1971, Ap. J. 169, 379.

Dakin, D.R., Tajima, T., Benford, G. and Rynn, N.: 1976, J. Plasma Phys. 15, 175.

Davidson, R.C.: 1972, Methods in Nonlinear Plasma Theory, Ch. 8,10,11 and 12, Academic Press (New York and London).

Davidson, R.C. and Ogdon, J.M.: 1975, Phys. Fluids 18, 1045.

Fried, B.D. and Gould, R.W.: 1961, Phys. Fluids 4, 139.

Ichimaru, S.: 1973, Basic Principles of Plasma Physics, Ch. 3 and 9, W.A. Benjamin Reading, Mass.

Ionson, J.A., Ong, R.S.B. and Fontheim, E.G.: 1979, Planet. Space Sci. 27, 203.

Kalfsbeek, H.W.: 1978, Rijnhuizen Reports 78-113 and 78-114.

Kaplan, S.A. and Tsytovich, V.N.: 1973, Plasma Astrophysics, Pergamon Press (Oxford).

Kindel, J.M. and Kennel, C.F.: 1971, J. Geophys. Res. 76, 3055.

Krall, N.A. and Trivelpiece, A.W.: 1973, Principles of Plasma Physics (New York: McGraw-Hill).

Lee, K.F.: 1972, J. Plasma Phys. 8, 379.

Manheimer, W.M. and Boris, J.P.: 1977, Comments on Plasma Physics and Controlled Fusion 3, 15.

Manheimer, W.M.: 1977, Phys. Fluids 20, 265.

Palmadesso, P.J., Coffey, T.P., Ossakow, S.L., Papadopoulos, K.: 1974, Geophysical Res. Lett. 1, 105.

Papadopoulos, K.: 1977, Rev. Geophys. Sp. Phys. 15, 113.

Petviashvili, V.I.: 1964, Sov. Phys. -JETP. 18, 1014.

Rosner, R., Golub, L., Coppi, B. and Vaiana, G.S.: 1978, Ap. J. 222, 317.

Schnack, D. and Killeen, J.: 1978, Theoretical and Computational Physics (IAEA, Vienna), p. 337.

Sivukhin, D.V.: 1966, Reviews of Plasma Physics, Consultants Bureau, New York. vol. 4.

Smith, D.F. and Lilliequist, C.E.: 1979, Ap. J. 232, 582.

Speiser, T.W.: 1970, Planet. Space Sci. 18, 613.

Spicer, D.S.: 1976, NRL report 8036.

Spicer, D.S.: 1980, to appear in Solar Physics.

Spitzer, L.: 1962, Physics of Fully Ionized Gases, Ch. 5, Interscience, New York.

Tange, T. and Ichimaru, S.: 1974, J. Phys. Soc. Japan, 36, 1437.

FIGURE CAPTIONS

Figure 1A: Critical drift speeds for ion-cyclotron waves (v_{IC}) and ion-acoustic waves (v_{IA}) as a function of the temperature ratio T_e/T_i. Also, v_{IC} v_{IA} are normalized to the electron thermal speed $v_e = (k_B T_e/m)^{\frac{1}{2}}$. The numbers 1, 2, 3 and 4 denote the different heating stages (see also Figure 2). For $T_e/T_i < 8$ ion-cyclotron waves have the lower threshold while for $T_e/T_i > 8$ ion acoustic waves are the first to go unstable.

Figure 1B: Fraction of the turbulently dissipated energy that goes into the electrons for ion-cyclotron waves (χ_{IC}) and ion-acoustic waves (χ_{IA}) under marginally stable conditions.

Figure 2: Computation of the drift velocity and the component resistivities in the four different plasma stages. An affirmative answer to the question posed in each stage, except the fourth, implies the switch-over to the next stage. The diagram pre-supposes $T_e/T_i < 8$ and does not continue beyond saturation of ion acoustic waves. For $T_e/T_i > 8$ in stage 1 the diagram is different in that ion-acoustic waves are th first to be excited. Inertial resistivity is included by replacing η_{CL} by $(\eta_{CL} + \eta_{IN})$. The symbols and expressions used are explained in the main text and Appendix II. The superscript s denotes the value at saturation.

Note that for the calculation of η's and w's at a given time, the previous history of the plasma is immaterial.

Figure 3: The value of the electron to ion temperature ratio when the current first becomes electrostatically unstable, is shown as a function of the growth rate of the electric field γ, for three different values of the filling factor ϵ. $(T_e/T_i)_{cr}$ is found numerically by solving the temperature equations in the classical phase until instability sets in.

Figure 4: Illustration of the evolution of the plasma in a drift velocity diagram for three different ion-cyclotron saturation levels: (A) a low saturation level due to plateau formation (Petviashvili, 1964); (B) $w_{IC}^{s} = 0.5$; (C) $w_{IC}^{s} = 0.01$. The dashed lines are the critical drift speeds of Figure 1A. The current layers are assumed to be large (formally $L \to \infty$), so that inertial resistivity is not important ($\eta_{IN} = 0$).

Figure 5: The low saturation case of Figure 4A in more detail. Time is in units of the growth time of the electric field, which for our choice of parameters is 0.7 sec.

Figure 6: The evolution of the plasma in a drift velocity diagram, with inertial resistivity dominant ($\eta_{IN} \neq 0$). Three different length scales L of the current layers are considered. (A) L = 3 km; $w_{IC}^{s} = 0.01$; (B) L = 1 km, $w_{IC}^{s} = 0.5$; (C) L = 10 km, $w_{IC}^{s} = 0.5$. Again the dashed lines are the critical drift speeds of Figure 1A.

Figure 7: The L = 3 km, $w_{IC}^{s} = 0.01$ case of Figure 6A in more detail. Time is in units of the growth time of the electric field, that is in units of 0.7 sec.

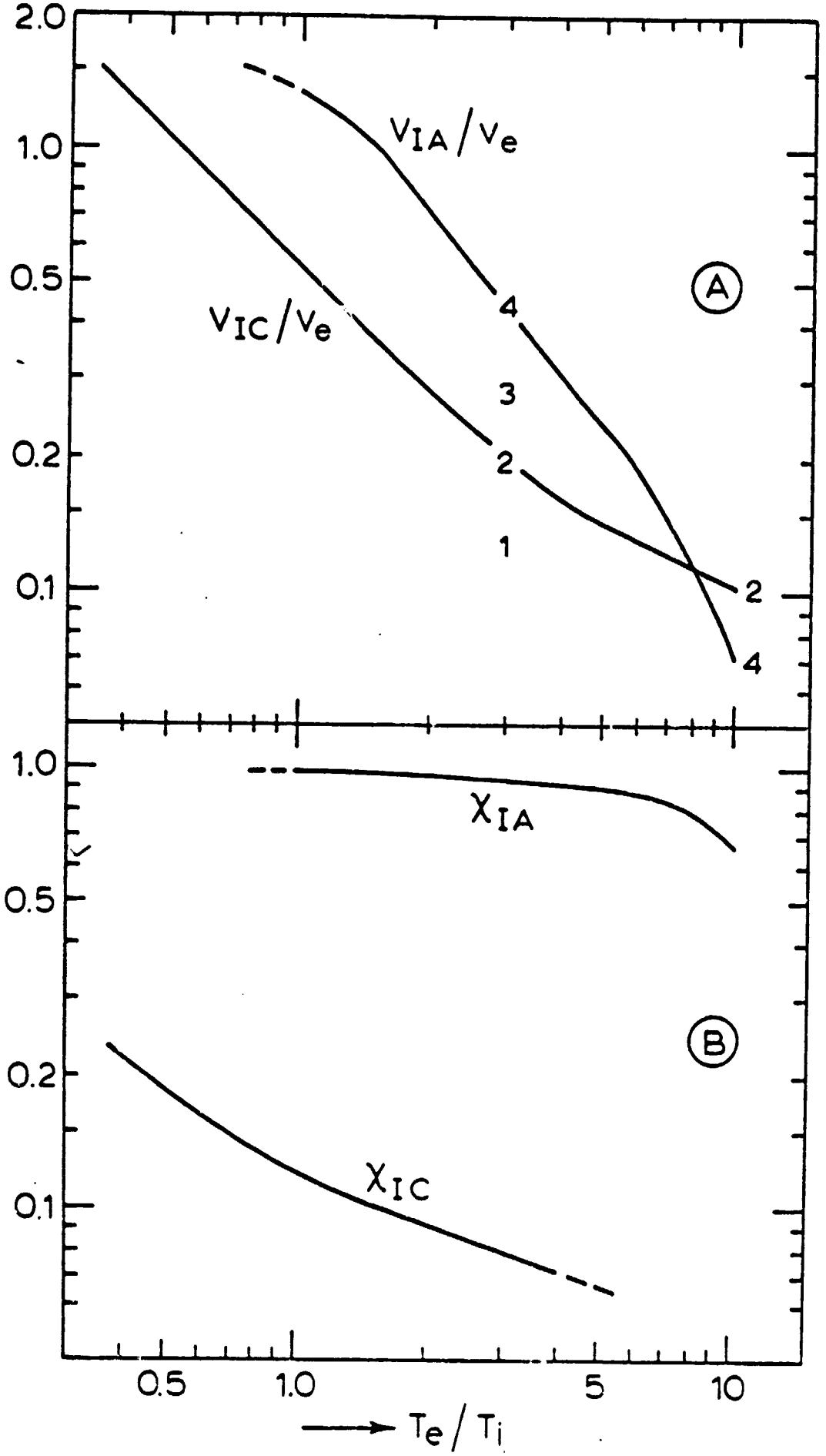
2.0
1.0
0.5
0.2
0.1
V_{IA}/V_e
V_{IC}/V_e
4
3
2
1
2
4
A
1.0
0.5
0.2
0.1
χ_{IA}
χ_{IC}
B
0.5
1.0
5
10
T_e/T_i

Figure 1

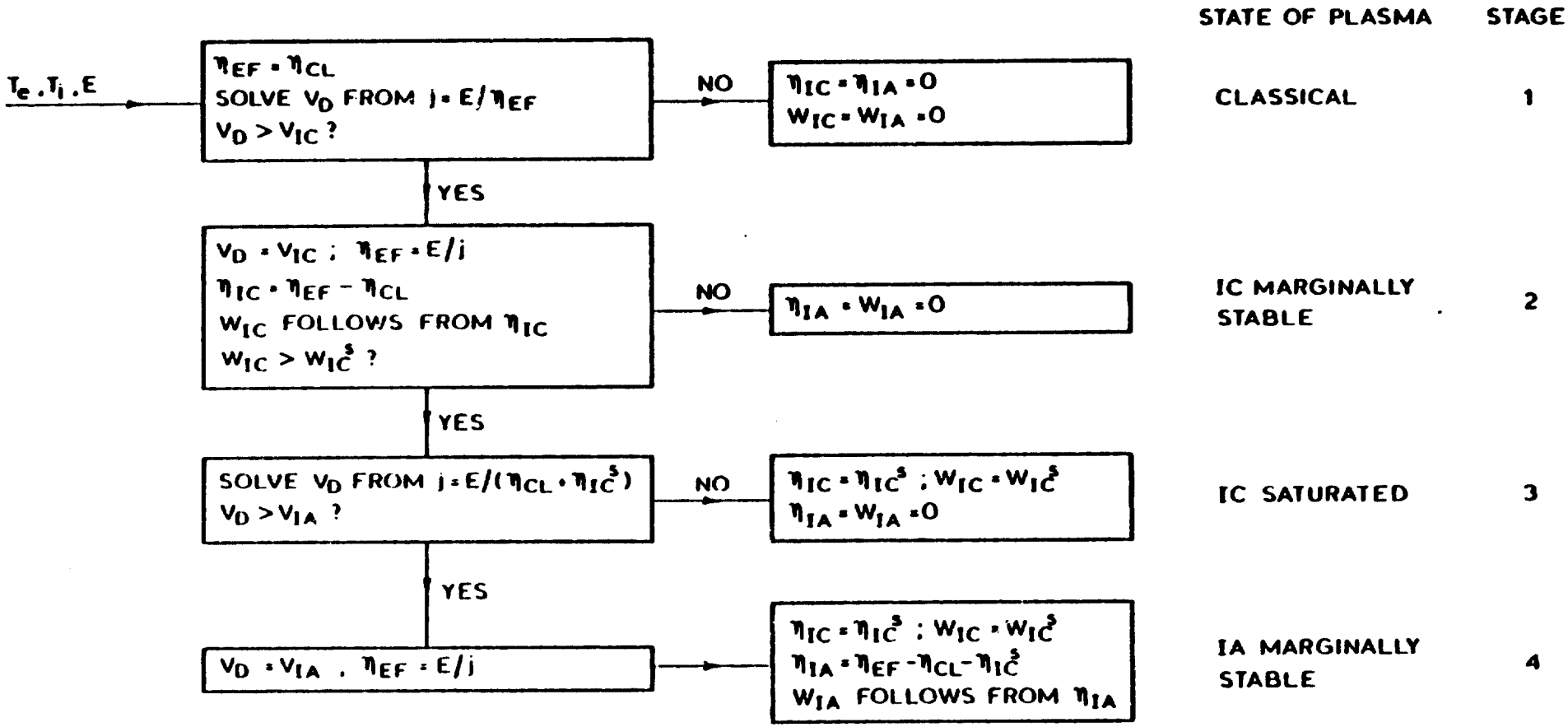
STATE OF PLASMA
STAGE
T_e, T_i, E
$\eta_{EF} = \eta_{CL}$
SOLVE V_D FROM $j = E/\eta_{EF}$
$V_D > V_{IC}$?
NO
$\eta_{IC} = \eta_{IA} = 0$
$W_{IC} = W_{IA} = 0$
CLASSICAL
1
YES
$V_D = V_{IC}$; $\eta_{EF} = E/j$
$\eta_{IC} = \eta_{EF} - \eta_{CL}$
W_{IC} FOLLOWS FROM η_{IC}
$W_{IC} > W_{IC}^S$?
NO
$\eta_{IA} = W_{IA} = 0$
IC MARGINALLY STABLE
2
YES
SOLVE V_D FROM $j = E/(\eta_{CL} + \eta_{IC}^S)$
$V_D > V_{IA}$?
NO
$\eta_{IC} = \eta_{IC}^S$; $W_{IC} = W_{IC}^S$
$\eta_{IA} = W_{IA} = 0$
IC SATURATED
3
YES
$V_D = V_{IA}$, $\eta_{EF} = E/j$
$\eta_{IC} = \eta_{IC}^S$; $W_{IC} = W_{IC}^S$
$\eta_{IA} = \eta_{EF} - \eta_{CL} - \eta_{IC}^S$
W_{IA} FOLLOWS FROM η_{IA}
IA MARGINALLY STABLE
4

Figure 2

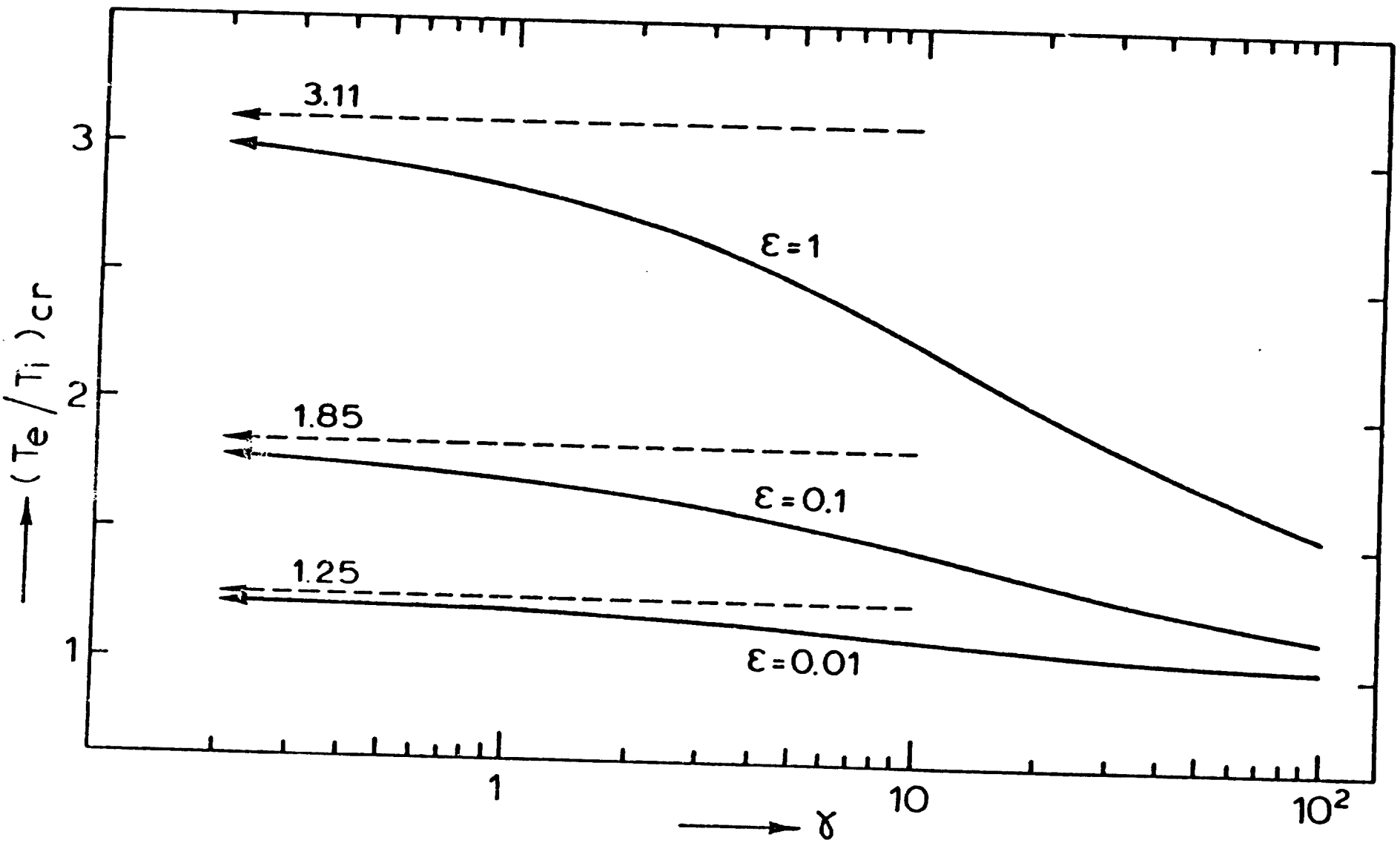
3.11
1.85
1.25
ε=1
ε=0.1
ε=0.01
3
2
1
(Te/Ti)cr
1
10
10²
γ

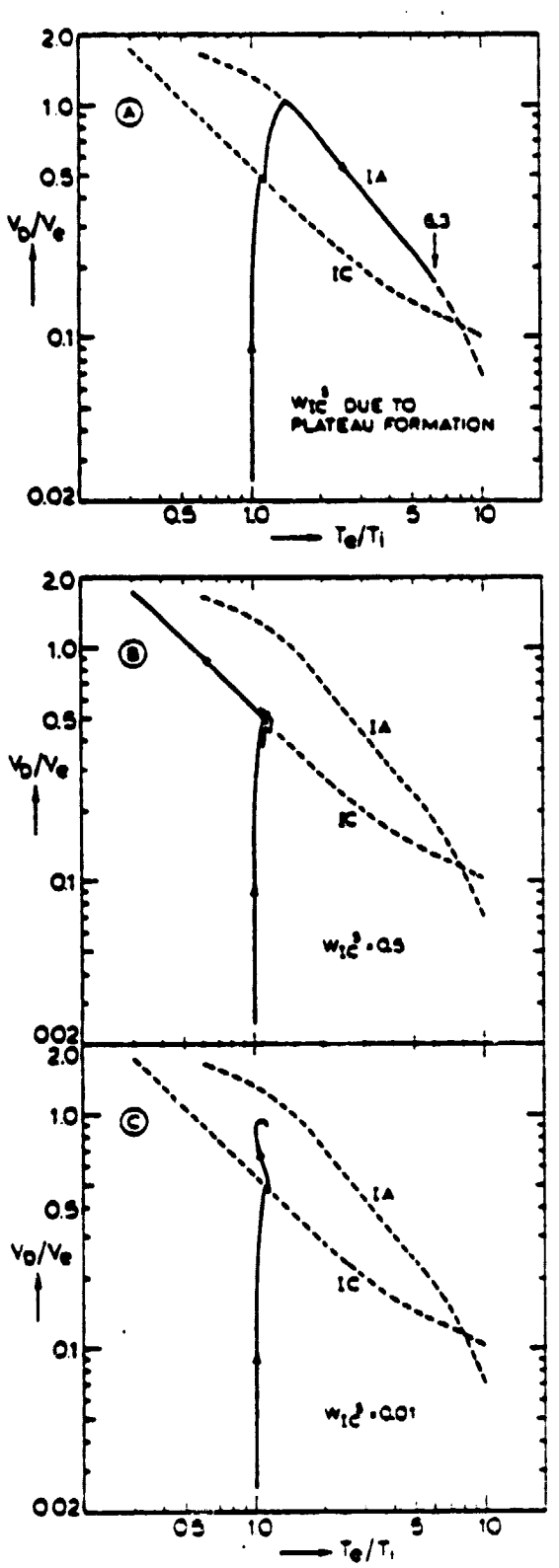

FIGURE 4

$\eta_{IN} = 0$

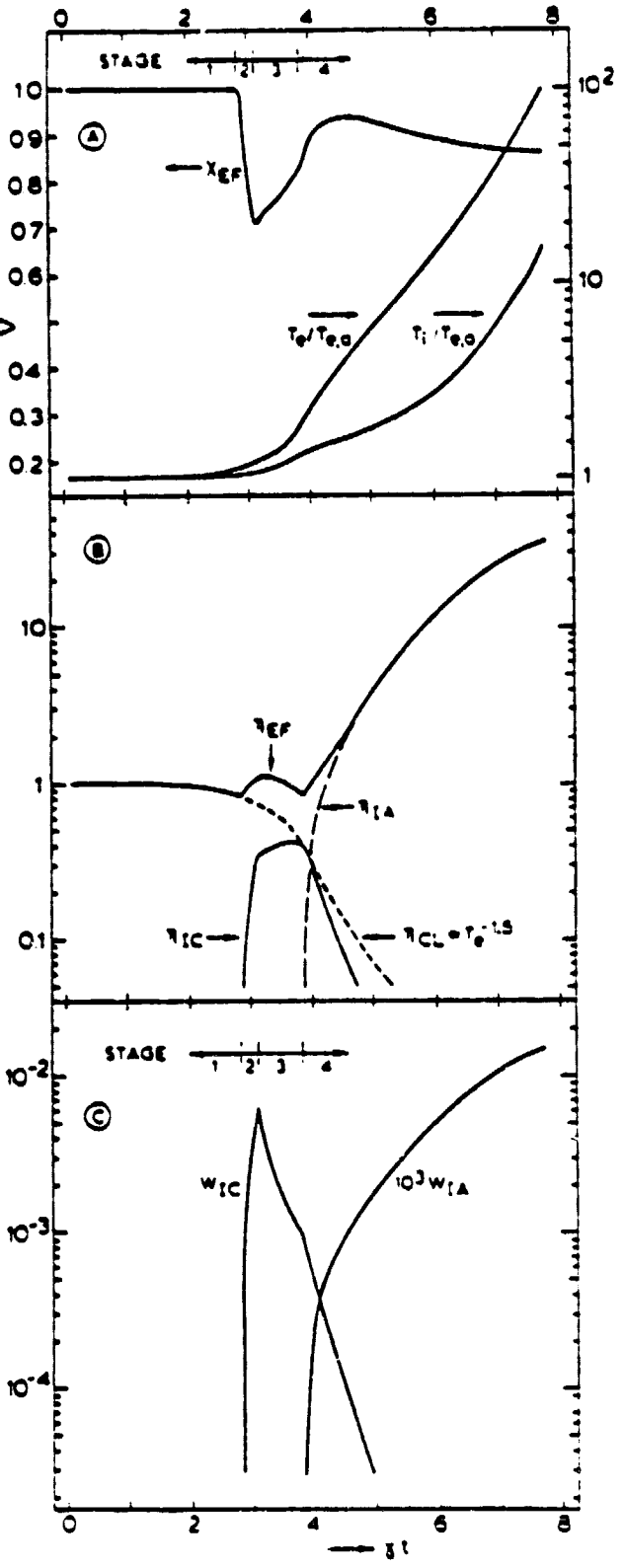

FIGURE 5

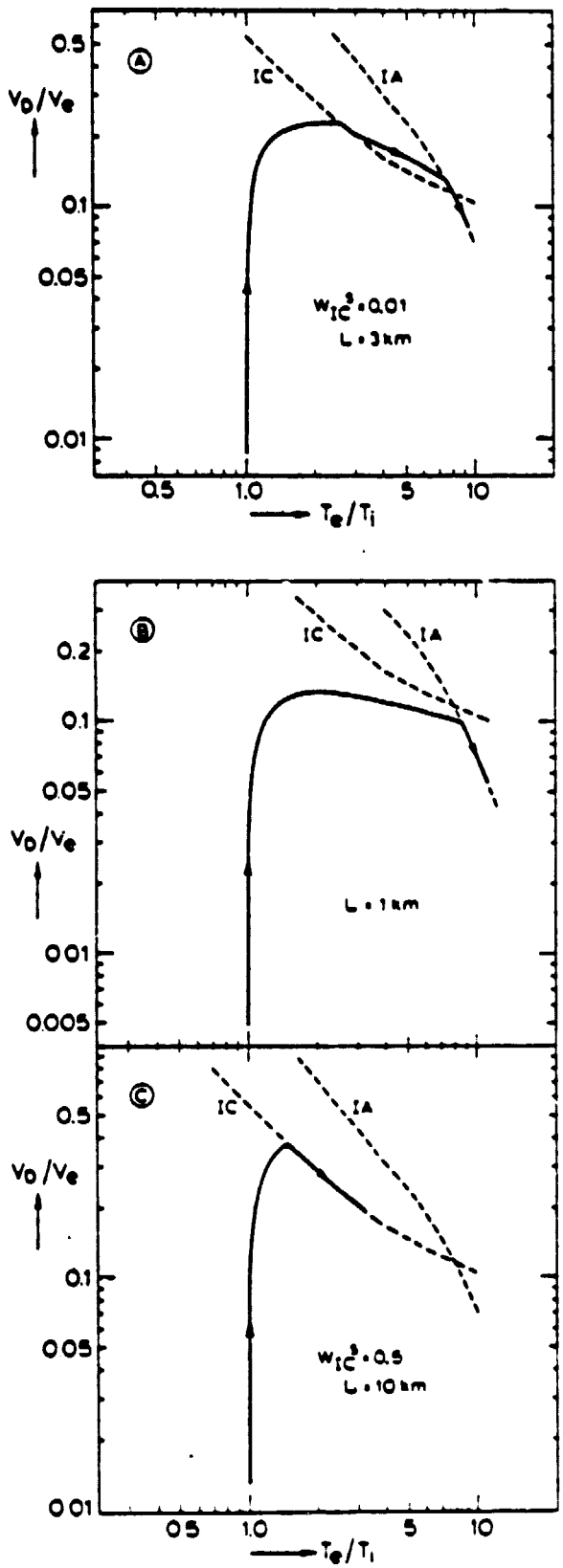

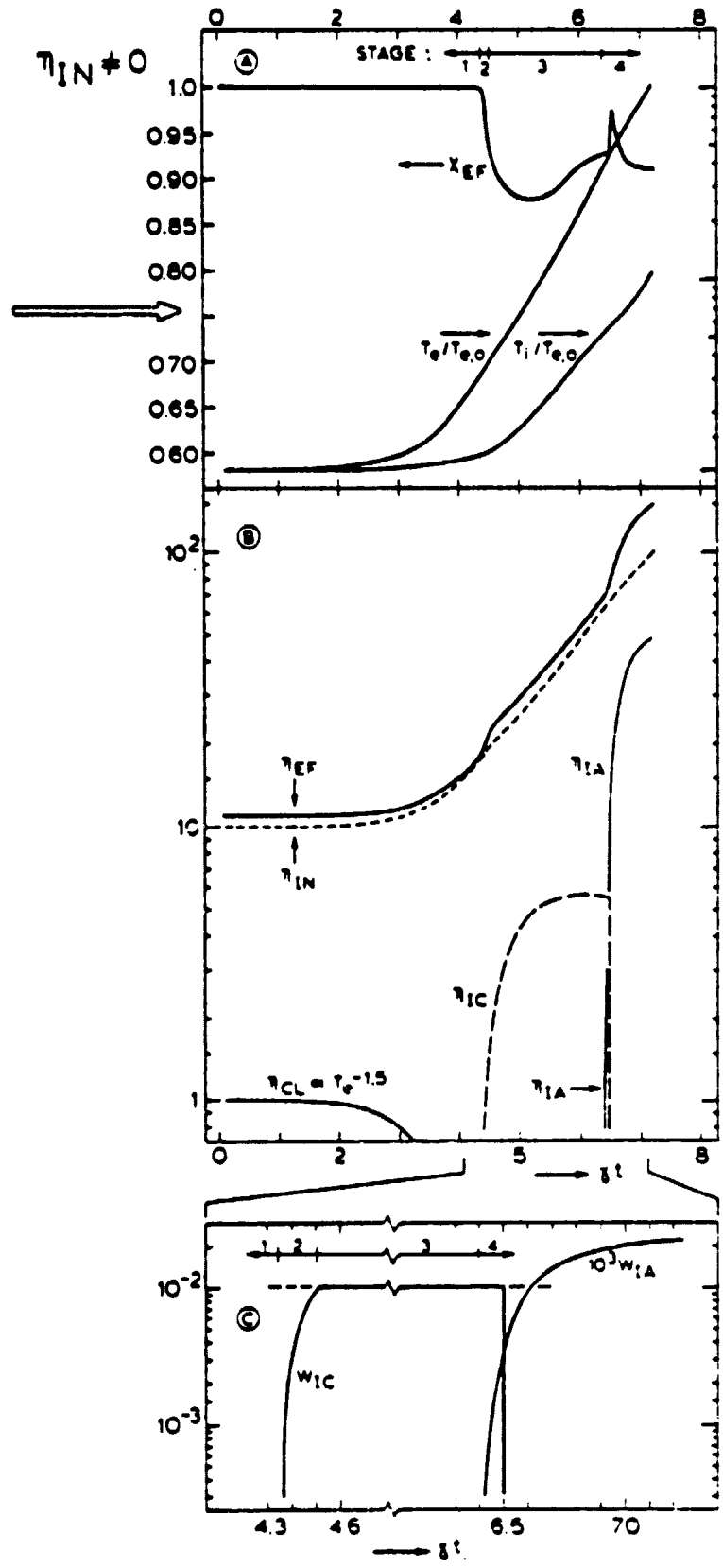

Figure 6

Figure 7